



Research Article

Elaboration and characterization of P3HT–PEO–SWCNT fibers by electrospinning technique

D. Hernández-Martínez¹ · M. E. Nicho² · G. Alvarado-Tenorio² · S. García-Carvajal² · M. M. Castillo-Ortega¹ · C. Vásquez-López¹

Received: 29 October 2019 / Accepted: 17 February 2020 / Published online: 21 February 2020
© Springer Nature Switzerland AG 2020

Abstract

In the present work, we report the preparation by the electrospinning technique and the characterization of poly(3-hexylthiophene)–polyethylene oxide–single wall carbon nanotubes (P3HT–PEO–SWCNT) fibers. The SWCNT concentration into the P3HT–PEO matrix is varied from 0.2 to 1%. Optical, electrical, thermal, and morphological properties of the P3HT–PEO–SWCNT fibers are determined. The incorporation of the SWCNT into the P3HT–PEO polymer matrix is determined by SEM, EDS analysis, TEM, FTIR, and Raman. The optical properties are analyzed by the determination of photoluminescence and photoresponse. The stability and degradation temperature of the fibers are determined by TGA. The morphology of the P3HT–PEO–SWCNT fibers depends on the SWCNT concentration, in all cases non-beaded fibers are obtained. It is found that the SWCNT incorporating into the P3HT–PEO fibers increases the conjugation length of P3HT chains. Charge transfer from P3HT to SWCNT is corroborated by photoluminescence and Raman. The P3HT–PEO–SWCNT fibers obtained in this work exhibit interesting optoelectronic properties that could be useful for device applications.

Keywords Composite · Poly(3-hexylthiophene) · Single wall carbon nanotubes · Electrospinning · Conductance

1 Introduction

Conjugated polymers have been extensively researched over several decades due to their enormous potential for several applications, including corrosion inhibitors, energy storages, optoelectronic devices and sensors [1]. The poly(3-alkylthiophenes) (P3AT) belonging to the conductive polymers are composed of monomer units of thiophene rings substituted in the 3-position with alkyl groups. Within the P3AT, the poly(3-hexylthiophene) (P3HT) has become one of the most widely studied conjugated polymers for applications in polymeric transistors and photovoltaic devices due to its high optoelectronic performance and easy processability.

The electrospinning technique is based on electrostatic forces forming microfibers to nanofibers. The force induces stretching and alignment of the polymer chains, as well as coalignment of carbon nanotubes (CNT) [2]. There are several reported techniques for fiber alignment; Cai et al. [3], used a collector of different geometry (U) to produce long, aligned fibers. Katta et al. [4], used copper wires in the form of a circular drum as collector which allows to obtain aligned fibers widely manipulated. Lei et al. [5], used a collector with parallel plates connected negatively, this collector allows to obtain well aligned fibers of great length. Recently, works on the molecular orientation along the fiber have been carried out. Kakade et al. [6], have investigated that the molecular orientation induced by an electric field can be performed, which produces a high

✉ D. Hernández-Martínez, diego.hernandez@unison.mx | ¹Departamento de Investigación en Polímeros Y Materiales, Universidad de Sonora, 83000 Hermosillo, Sonora, Mexico. ²Centro de Investigación en Ingeniería y Ciencias Aplicadas, Universidad Autónoma del Estado de Morelos (UAEM), Av. Universidad 1001, Col. Chamilpa, C.P. 62210 Cuernavaca, Morelos, Mexico.



degree of orientation of the main polymer chains along the fiber axis. Bounioux et al. have studied the effects of the CNT dispersion in P3AT and the preparation of single wall carbon nanotubes (SWCNT)–phenyl-C61-butyric acid methyl ester (PCBM)–P3HT fibers via electrospinning [2, 7, 8], finding the feasibility for optoelectrical applications.

CNT, including multiwalled carbon nanotubes (MWCNT) have recently attracted considerable research interest due to its electrical properties [1]. CNT have excellent mechanical properties and good electrical and thermal conductivity, making CNT an ideal material for reinforcing polymer materials [9]. Advantages of CNT-based nanocomposites over conventional polymer composites are due to the fact that the large surface areas of the CNT facilitates a better interfacial interaction [10, 11]. The properties of these polymeric nanocomposites depend largely on the dispersal capacity of nanofillers [12].

Dror et al. [13] and Salalha et al. [14] studied the orientation of MWCNT into the MWCNT/poly(ethylene oxide) (PEO) fibers, MWCNT were embedded in a straight and aligned form. Ren et al. [15], reported the use of P3HT/s-SWCNT nanofilaments in the solar cells active layer, absorption and quenching of the PL indicated significant interactions among the components and good electrical properties, they demonstrated that P3HT/s-SWCNT heterojunction can generate photocurrent of absorbed photons in both P3HT and s-SWCNT and achieve 26% near-infrared internal quantum efficiency (IQE). Bar-Hen et al. [16], reported the electrospinning of fibers composed of P3HT, fullerene derivative, phenyl-C61-butyric acid methyl ester (PCBM), and SWCNT. They found a high degree of ordering and alignment within the fibers, significant interactions among the components, and strong photoluminescence quenching that points out to the efficient charge transfer in these nanocomposites.

In this work, the preparation by electrospinning technique and characterization of P3HT–PEO–SWCNT fibers were reported. Optical, electrical, thermal, and morphological properties of the P3HT–PEO–SWCNT fibers were determined. Raman analysis was carried out for determining the structure of composites.

2 Experimental

2.1 Materials

For the synthesis of P3HT, the following reagents were used: 3-hexylthiophene monomer (Aldrich), FeCl₃ (97%) (Aldrich), methanol (Fermont), chloroform (Baker), hydrochloric acid (Baker), acetone (Baker), ammonium hydroxide (10%), EDTA (1%). Fiber formation: PEO (Mw = 1,000,000, Sigma-Aldrich) and chloroform (Sigma-Aldrich).

SWCNT (80% SWCNT, external diameter = 1–2 nm, length = 5–15 μm) were purchased from Nanostructured & Amorphous Materials Inc., and Acetonitrile (99%, Sigma-Aldrich) for washing.

2.2 Synthesis of P3HT

P3HT was chemically synthesized at 0 °C using FeCl₃ as oxidant under nitrogen atmosphere, following a procedure reported in previous work [17]. The final P3HT product showed Mn = 62,365 g/mol, Mw = 256,454 g/mol; PDI = 4.1 estimated by GPC.

2.3 Preparation of P3HT–PEO–SWCNT fibers by electrospinning

The electrospinning solution was prepared by dissolving P3HT (80 wt%) and PEO (20 wt%) in chloroform solvent [17]: P3HT solution in chloroform was stirred for 15 min, then PEO dissolved in chloroform was added and the polymer mix was stirred for 20 min until that the solution was homogeneous. Additionally, P3HT–PEO–SWCNT electrospinning solution was prepared, the SWCNT concentration was varied in the P3HT–PEO solution (0.2, 0.4, 0.6, 0.8 and 1% weight). The SWCNT were previously ultrasounded for 30 min, and subsequently dispersed by sonication in CHCl₃ for 24 h. When the dispersion was homogeneous, P3HT and PEO solutions in CHCl₃ previously stirred during 30 min, were added to the SWCNT solution, then sonicated by 5 min and stirred during 30 min. According to Samanta et al. [18] and Francis et al. [19] the sonication-assisted dispersion of CNT in P3AT solutions proceeds by adsorption of the polymers from solution onto the CNT.

A syringe filled with the P3HT–PEO–SWCNT solution was placed in an injection pump (NEW ERA NE-300) connected to a voltage source (CZE1000R Spellman). Electrospinning parameters: flow rate = 3.2 mL/h, applied voltage = 11 kV, and the distance from the tip of the needle to the collector = 24 cm. The formed fibers were deposited on an aluminum collector plate of 15 cm².

3 Characterization

Dyads configuration was determined by proton nuclear magnetic resonance (Varian Inova 400 instrument) using deuterated chloroform as solvent. Elemental content and morphology of P3HT–PEO and P3HT–PEO–SWCNT fibers were characterized by scanning electron microscopy (Hitachi SE-SEM 5500) equipped with an energy-dispersive X-ray analysis system, and TEM JEOL jerm-2010f. FTIR spectra of the fibers were recorded in a Perkin Elmer LR64912C FTIR-ATR spectrophotometer. Raman spectra

of RBC were acquired with a Raman microspectrometer (Witec, alpha300 RA, Ulm, Germany) using a frequency doubled Nd: YAG laser excitation of 532 nm (CW—continuous wave). Raman measurements were carried out with 10 s of accumulation time, 3 acquisition and 10mW of laser power. Thermal stability and decomposition temperature of the fibers were determined by thermogravimetric analysis (TGA TA Q500); the samples were measured in nitrogen atmosphere and heated at 10 °C/min rate. The samples were measured by photoluminescence in a fluorospectrometer (LAMBDA 650, Perkin Elmer) at an excitation wavelength of 450 nm. Finally to obtain the photoresponse data, a 100 mW Oriel Xenon lamp was used, placing the electrodes directly on the fibers, separated at a distance of 0.5 cm, 1 V voltage was applied, with measurement intervals 20 s in dark and 20 s in light.

4 Results and discussion

4.1 ^1H NMR analysis

Figure 1 shows the ^1H NMR spectra of P3HT, the signal of 7.2 ppm corresponds to deuterated chloroform, the signals between 2.5–3.0 ppm corresponds to CH_2 , which is attached to the thiophene ring (f), the signal at 2.8 ppm, corresponds to one of the dyads head–tail union (HT) and the 2.56 ppm corresponds to the head–head joint (HH). Signals between 6.9 and 7.1 ppm correspond to the proton in position four of the thiophene ring [20], the signal at 6.98 ppm corresponds to the head/tail–head/tail (HT–HT) triad, the signal at 7.0 ppm corresponds to the head/tail–head/head (HT–HH) triad, the signal at 7.02 ppm corresponds to the tail/tail–head/tail (TT–HT) triad, and finally the signal to 7.05 ppm corresponds to the tail/tail–head/head (TT–HH) triad. The P3HT showed 88% of HT dyads.

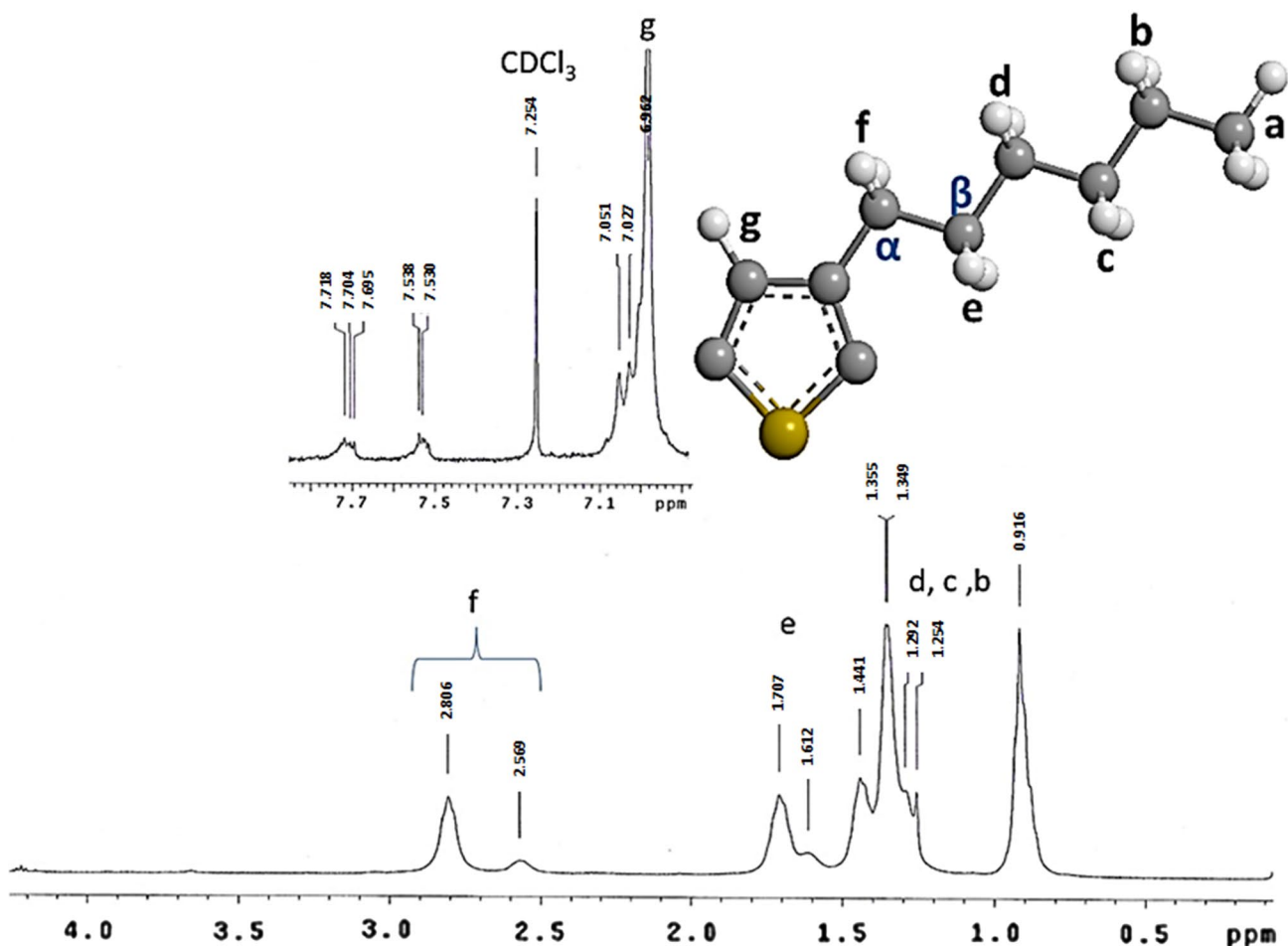


Fig. 1 ^1H NMR Analysis of P3HT

4.2 Morphology of P3HT–PEO–NTCS fibers

Figure 2 shows the morphology of electrospun P3HT–PEO (Fig. 2a, b) and P3HT–PEO–SWCNT (Fig. 2c–l) fibers. The morphology of the P3HT–PEO fibers is porous with heterogeneous pore size, the fibers showed an average diameter of 3.75 μm . The morphology of the P3HT–PEO–SWCNT fibers depended on the SWCNT concentration. The fibers showed an average diameter in the range of 3.05 to 4.16 μm , in all cases fibers without beads were obtained. The most homogenous dimensions were obtained for the P3HT–PEO–SWCNT fibers with 0.6% of SWCNT. A greater amplification (Fig. 2d, f, h, j, l) shows surface characteristics that depend on the SWCNT percentage into the P3HT–PEO fibers. The P3HT–PEO–SWCNT fibers with a low concentration of nanotubes (0.2 and 0.4%) are porous and show very heterogeneous surface features on the fibers surface. When the amount of NTCs increases to 0.6%, the pore size decreases and a more homogeneous morphology is presented with some ordering in the transversal sense of the fiber (as a ringed morphology). However, when the nanotubes concentration continues to increase to 0.8% (Fig. 2j), a homogeneous morphology like ridges with ordering in the longitudinal direction of the fiber (morphology as channels) is observed and the porosity continued diminished. Finally when reaching 1% of nanotubes, the ridges are separated and between them appears the morphology shown by fibers with low nanotubes concentration. It is possible that the ridges and rings are due to the alignment of the nanotubes.

Saini et al., observed that as the concentration of MWNT increases, a weaker interaction between the nanotubes and the polymers is given by the poorer nanotubes dispersion in the polymer matrix, the increase in MWNT led to its agglomeration, it was found that they interact more strongly with each other and less with the polymers [21]. Probably for the P3HT–PEO–SWCNT fibers, from a concentration of 0.6% of nanotubes the agglomeration of the nanotubes is taking place.

In order to corroborate the carbon nanotubes content, EDS analysis was performed on the fibers, Table 1 shows the results. The carbon/sulphur (C/S) ratio in the P3HT–PEO fibers was 10.5, as it was expected when the SWCNT were incorporated to the P3HT–PEO fibers such ratio was increased. However at 0.8 and 1.0% of SWCNT, the C/S ratio decreased compared to the fibers with lower concentrations of SWCNT, probably at those concentrations, the nanotubes were agglomerated inside the fiber, displacing the polymer towards the outside of the fiber.

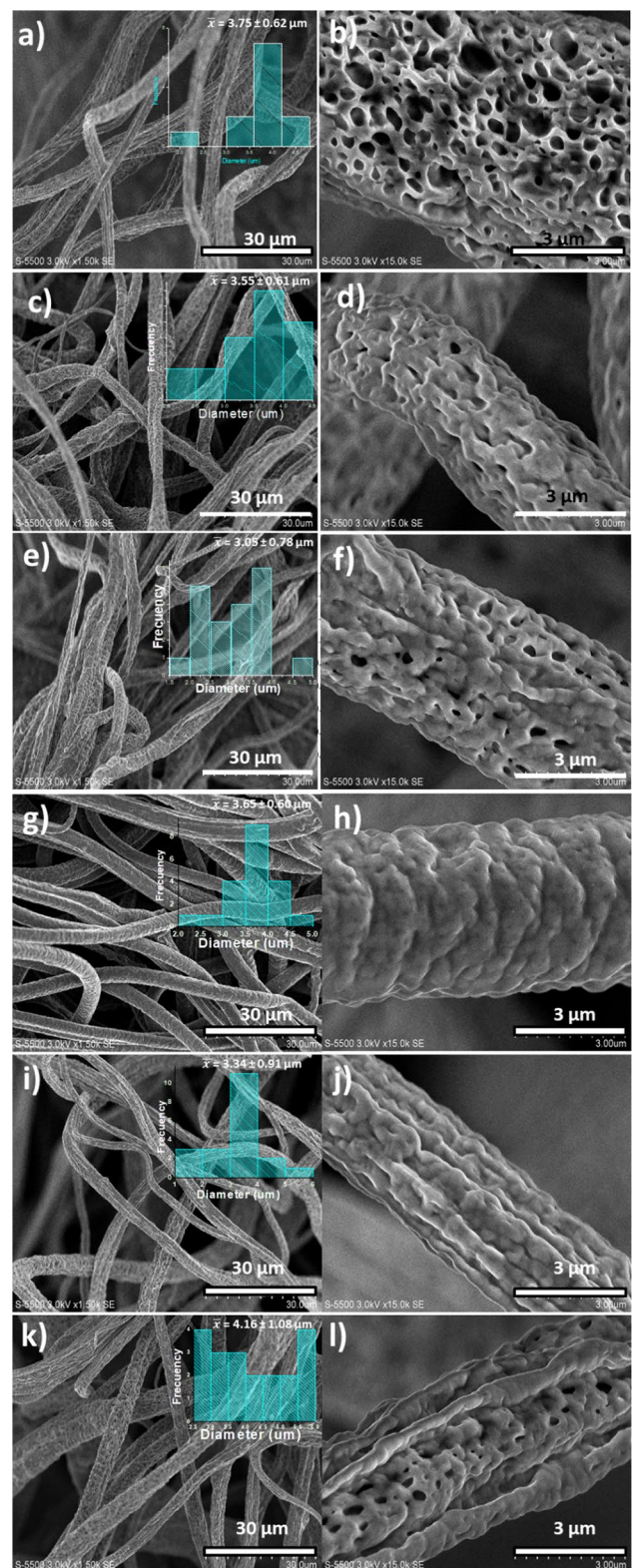
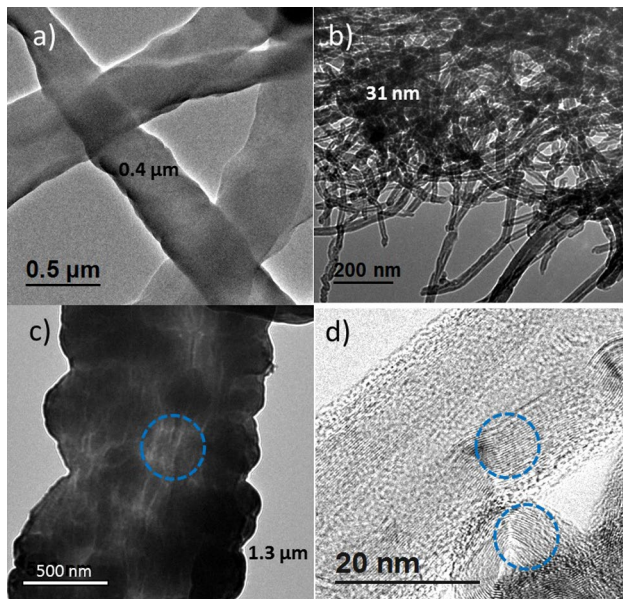


Fig. 2 SEM images of P3HT–PEO fibers with different concentrations of SWCNT: **a** and **b** 0%, **c** and **d** 0.2%, **e** and **f** 0.4%, **g** and **h** 0.6%, **i** and **j** 0.8%, **k** and **l** 1%. Inset figures **a**, **c**, **e**, **g**, **i**, and **k** corresponds to the fibers diameter distributions

Table 1 C/S atom (%) ratio in P3HT–PEO fibers with different concentrations of SWCNT obtained by the EDS analysis

SWCNT (%)	Element	wt% weight	wt% atomic	Atomic ratio C/S
P3HT	C	77.02	86.49	10.5
	S	19.38	8.16	
0.20%	C	65.83	83.72	10.7
	S	34.17	7.8	
0.40%	C	86.51	94.48	17.1
	S	13.49	5.52	
0.60%	C	91.9	96.81	30.3
	S	8.1	3.19	
0.80%	C	89.78	95.91	23.4
	S	10.22	4.09	
1.00%	C	88.11	95.19	19.8
	S	11.89	4.81	

**Fig. 3** Images (TEM): **a** P3HT–PEO–SWCNT fibers with 0.4% of SWCNT, **b** CNT, **c** and **d** part of P3HT–PEO–SWCNT fiber

4.3 TEM analysis

Figure 3 shows the TEM micrographs of the P3HT–PEO–SWCNT fibers with 0.4% of SWCNT (Fig. 3a), pristine SWCNT (Fig. 3b), and part of P3HT–PEO–SWCNT fiber (Fig. 3c, d), 3d bright field TEM image. In Fig. 3c, d, the alignment of the nanotubes in longitudinal orientation of the fiber was observed. The accumulation and alignment of the SWCNT are observed as a fingerprint (circles marked in Fig. 3d). SWCNT have diameter size approximately between 5 and 50 nm and are forming clusters in

different parts of the fibers. A high degree of ordering and alignment within the P3HT–PCBM–SWCNT fibers was also observed by Bounioux et al. [2]. Probably by increasing the SWCNT concentration in the P3HT–PEO solution, the strong Vander Waals interaction between the nanotubes increases, and they begin to align locally in the same direction forming aggregates [22].

4.4 TGA analysis

TGA graphs of the SWCNT, P3HT and P3HT–PEO–SWCNT composite fibers are shown in Fig. 4. The maximum decomposition temperature of P3HT film was given at 494 °C, and for the carbon nanotubes at 558 °C. The P3HT–PEO fibers showed two maximum decomposition temperatures, at 392 °C due to PEO decomposition, and 474 °C due to P3HT decomposition [17]. The P3HT–PEO–SWCNT fibers also showed two decomposition temperatures: 404 °C and 488 °C for fibers with 0.2% of nanotubes, 396 °C and 483 °C for fibers with 0.4% of nanotubes, 404 °C and 489 °C for fibers with 0.6% of nanotubes, 387 °C and 483 °C for fibers with 0.8% of nanotubes, and 385 °C and 469 °C for fibers with 1.0% of nanotubes. The first one decomposition temperature is related to the decomposition of PEO and the second one related to decomposition of P3HT [17]. The P3HT–PEO–SWCNT fibers showed lower degradation temperature and thermal stability than P3HT. In comparison with the P3HT–PEO fibers, the thermal stability of P3HT–PEO–SWCNT fibers was lower, however, the decomposition temperature depended on the nanotubes concentration. At a SWCNT concentration higher than 0.6%, lower decomposition temperature of both PEO and P3HT. In the P3HT–PEO–SWCNT fibers with 0.8% and 1.0% of nanotubes, the decomposition of the nanotubes starts at a temperature of 630 °C. The loss of the SWCNT within the composites fibers is carried out at a higher temperature, probably due to their interaction with the polymers. Similar results were obtained for SWCNT/P3OT composites synthesized by in-situ chemical oxidative microwave-assisted polymerization [23].

4.5 FTIR spectroscopy

The FTIR spectra of SWCNT, P3HT and P3HT–PEO–SWCNT fibers are shown in Fig. 5. The P3HT–PEO fibers exhibited the characteristic bands of P3HT and PEO. P3HT characteristic bands showed by the fibers: 722 cm^{-1} methylene groups rock, 820 cm^{-1} aromatic C–H out-of plane vibration, 1114 cm^{-1} C–S stretching, the peaks at 1510 cm^{-1} and 1460 cm^{-1} corresponds to thiophene ring C=C stretching vibration, asymmetric and symmetric, respectively, 1377 cm^{-1} is due to methyl bending, three bands at 2954 cm^{-1} , 2920 cm^{-1} and 2852 cm^{-1} assigned to the

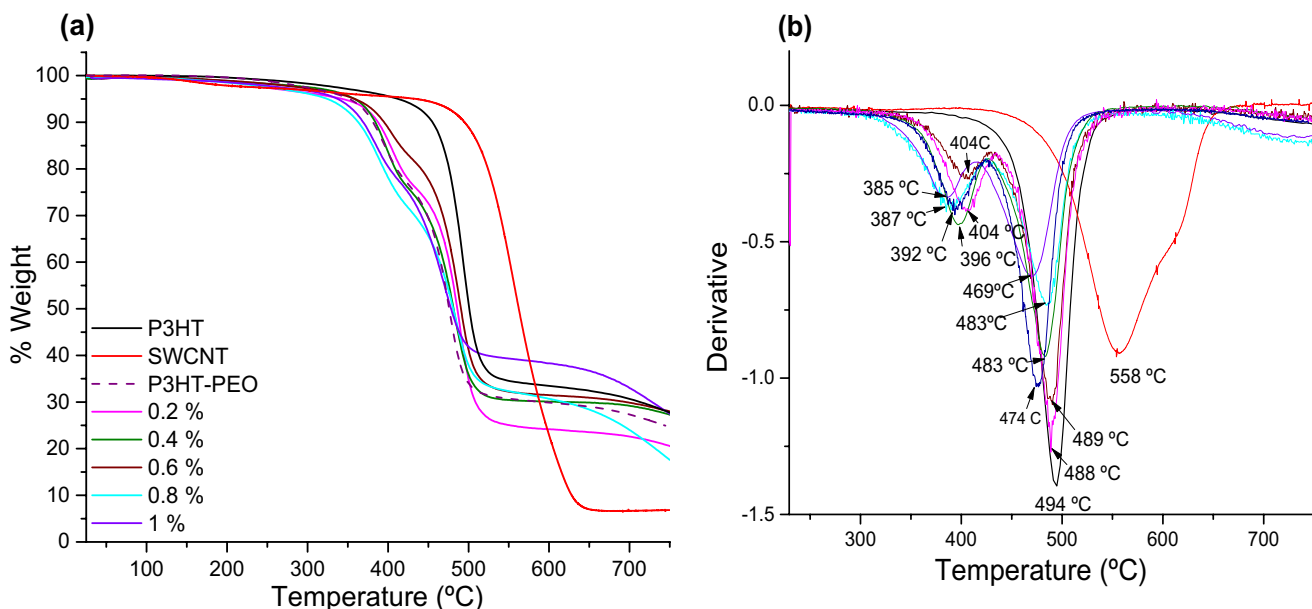


Fig. 4 TGA analysis of SWCNT, P3HT and P3HT-PEO-SWCNT fibers at different concentrations: **a** % weight versus temperature and **b** derivative versus temperature

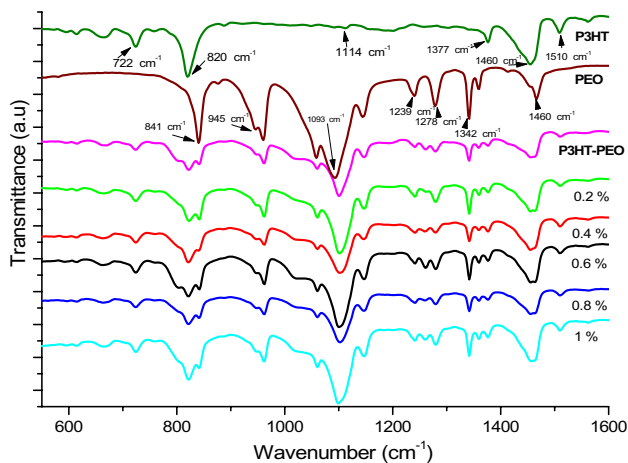


Fig. 5 FTIR spectra of P3HT, PEO and P3HT-PEO-SWCNT fibers; in the frequency range of 750–1600 cm^{-1}

asymmetric C–H stretching vibrations of CH_3 – moieties, $-\text{CH}_2$ – moieties, and symmetric C–H stretching vibration in $-\text{CH}_2$ – moieties, respectively [24–26]. PEO characteristic bands showed by the fibers: 1460 cm^{-1} and 1342 cm^{-1} CH_2 asymm. bending, 1278 cm^{-1} CH_2 twist, 1239 cm^{-1} , 1093 cm^{-1} C–O–C asymmetric stretch, 945 cm^{-1} CH_2 rock, C–O–C stretch, 841 cm^{-1} CH_2 asymm. Rocking [24–27].

The incorporation of the SWCNT in the composite is not clear, probably the percentage of the nanotubes is small which does not allow to appreciate the characteristic bands of the nanotubes. Probably the band at 1016 cm^{-1} is due to the incorporation of the nanotubes in the matrix

Table 2 $I_{\text{sym}}/I_{\text{asym}}$ ratio P3HT-PEO-SWCNT fibers

	$I_{\text{sym}}/I_{\text{asym}}$ ratio
Film P3HT	3.1
P3HT-PEO fiber	5.1
P3HT-PEO-SWCNT 0.2%	3.8
P3HT-PEO-SWCNT 0.4%	3.7
P3HT-PEO-SWCNT 0.6%	3.9
P3HT-PEO-SWCNT 0.8%	4.1
P3HT-PEO-SWCNT 1.0%	4.4

P3HT-PEO [28]. By incorporating the carbon nanotubes in P3HT-PEO, the intensity of the bands at 1510 cm^{-1} and 1460 cm^{-1} are increased, due probably to the interaction between the thiophene ring and the nanotubes. This increase in bands intensity at 1510 cm^{-1} and 1460 cm^{-1} was also observed by Musumeci et al. for a concentration of 0.1% MWNT in P3HT/MWNT composites, [29].

Higher conjugation length in the polymer backbone results in smaller $I_{\text{sym}}/I_{\text{asym}}$ ratio [30]. Table 2 shows the results of $I_{\text{sym}}/I_{\text{asym}}$ ratio for P3HT and P3HT-PEO fibers with different SWCNT concentration. The SWCNT incorporating into the P3HT-PEO fibers increased the conjugation length of the P3HT chains. At a lower concentration of SWCNT within the P3HT-PEO fiber, a greater conjugation length was obtained in the P3HT chains. This could be due to the fact that at higher concentrations of SWCNT in the fiber, these tend to agglomerate interfering with the arrangement of P3HT chains. However, the conjugation length

for all P3HT-PEO-SWCNT fibers was shorter compared to P3HT but longer than P3HT-PEO fiber.

4.6 Raman analysis

Raman analysis is sensitive to both electronic and vibrational structures of CNT, which can be used to probe the structure of composite [31]. The spectra of P3HT, SWCNT and P3HT-SWCNT fibers are shown in Fig. 6. The pristine SWCNT show a Raman spectrum containing a G band (1570 cm^{-1}) of sp^2 carbon, along with a D band (1336 cm^{-1}) of sp^3 carbon and a G' band (2678 cm^{-1}) of graphite [32]. P3HT has two peaks at 1376 and 1453 cm^{-1} , which are assigned to the C-C and C=C skeletal stretching vibration, respectively [33]. The peaks of the D and G bands in the composite were shifted to a higher wave number by 8 and 6 cm^{-1} , respectively. According to the literature, this change could be attributed to the strong interaction and to charge transfer between the polymer and SWCNT [15].

4.7 Photoluminescence analysis

Photoluminescence (PL) is commonly used as a first approximation to determine whether charge transfer occurs in heterojunctions, a decrease in PL signal is attributed to charge transfer from a photo-excited polymer to acceptor [34]. PL of P3HT-PEO and P3HT-PEO-SWCNT fibers was measured under excitation of 450 nm (Fig. 7). The incorporation of SWCNT into the P3HT-PEO fibers reduced the intensity of the PL (quenching). When 0.2% of nanotubes was added to the P3HT-PEO fiber, PL was reduced by approximately 78% and the spectrum was blue-shifted

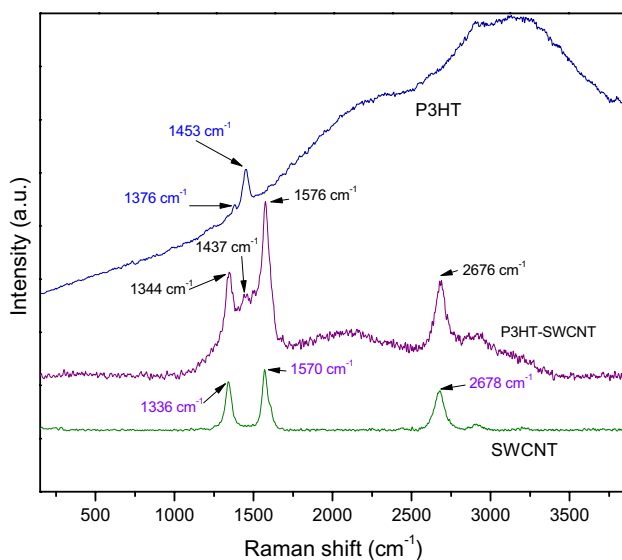


Fig. 6 Raman spectra of P3HT, SWCNT and P3HT-SWCNT fibers for excitation at 532 nm

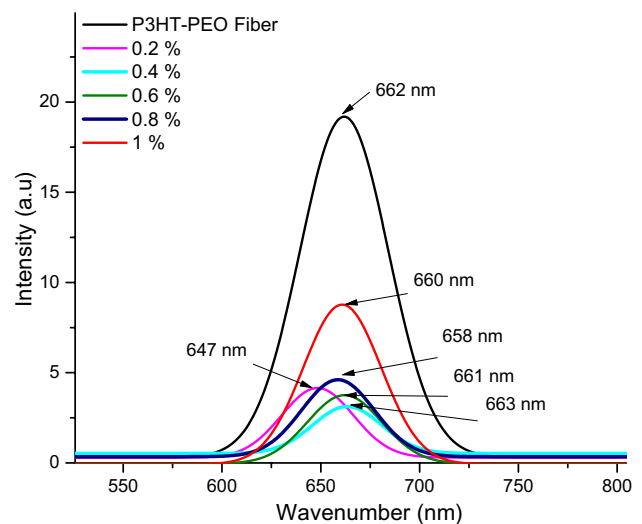


Fig. 7 Photoluminescence spectra at 450 nm for: P3HT/PEO and P3HT-PEO-SWCNT fibers

by 15 nm with respect to that of the P3HT-PEO fibers. By increasing the percentage of nanotubes to 0.4% , the PL decreased further, and the spectrum was red-shifted by 16 nm with respect to the P3HT-PEO fibers with 0.2% of SWCNT. The PL intensity decrease with the addition of SWCNT in P3HT has already been reported by Goutam et al. [35]. Likewise, Ren et al. reported the PL quenching in P3HT/s-SWCNT nanofilaments [15]. At a higher nanotubes concentration ($0.6, 0.8$ and 1%), the PL increased, the higher the concentration the greater PL. Probably the increased PL at these concentrations is due to the agglomeration of the nanotubes, what affects the order of the polymer chains. The PL quenching of the P3HT-PEO-SWCNT fibers suggests that well-ordered P3HT-PEO polymer layers into of the fiber form an intimate contact with the nanotubes and can improve the dissociation of the excitons generated in the P3HT [15]. The PL decrease is considered to be a non-radiative recombination due to the high interfacial area of the SWCNT with the polymer matrix, so the load transfer between the two phases is good.

The photoluminescence quenching of the P3HT-PEO-SWCNT fibers may be attributed to π - π interactions of P3HT with the nanotubes that form additional decaying paths for the excited electrons [33].

4.8 Photoresponse

Figure 8 shows the electrical conductance of P3HT-PEO fibers with different SWCNT concentration, and Table 3 shows the results electrical conductance in dark and lighting of the P3HT-PEO-SWCNT fibers. The P3HT-PEO-SWCNT fiber with 0.4% SWCNT showed the higher electrical conductance in both dark and illumination, which probably

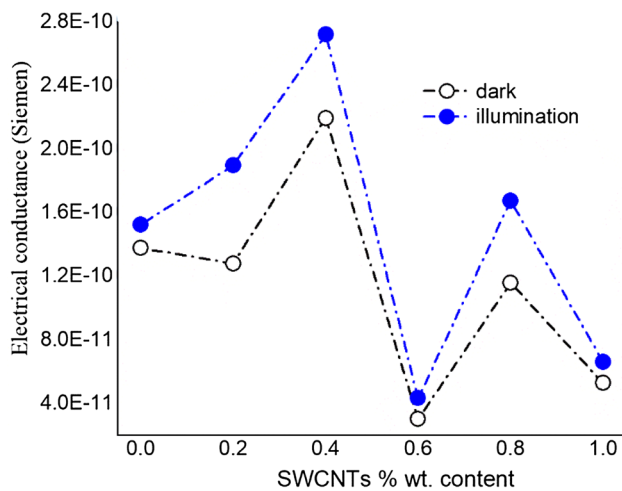


Fig. 8 Graph of electrical conductance versus SWCNT wt% in P3HT-PEO fibers

Table 3 Electrical conductance

Sample	SWCNT (wt%)	G_{dark} (Siemen)	G_{light} (Siemen)
P3HT/PEO (raw)	0	3.221E-11	4.795E-11
P3HT/PEO	0.2	1.2795E-10	1.897E-10
P3HT/PEO	0.4	2.1944E-10	2.72E-10
P3HT/PEO	0.6	3.001E-11	4.323E-11
P3HT/PEO	0.8	1.1584E-10	1.6746E-10
P3HT/PEO	1.0	5.264E-11	6.609E-11

indicates that at this concentration a better dispersion of the nanotubes within the polymer matrix is given. The fibers with 0.4% of nanotubes show a greater porosity on the surface (Fig. 2), probably the greater contact area between the CNT and P3HT benefits the conductivity of the material.

This behavior has already been reported by our group [23], where P3HT films with SWCNT were elaborated. Fibers with SWCNT concentration of 0.6%, 0.8% and 1% have electrical conductance values lower than or equal to the fiber without nanotubes, this suggests a recombination of the electrons photogenerated by increasing the SWCNT concentration.

5 Conclusions

P3HT-PEO-SWCNT fibers were prepared with different concentration of SWCNT by the electrospinning technique. The addition of CNT to the P3HT-PEO fibers modified their porous morphology, at a certain concentration it was possible to obtain a transverse or longitudinal order with ring-shaped or crested morphology, respectively. TEM

images showed alignment and aggregation of the nanotubes in longitudinal orientation of the P3HT-PEO-SWCNT fiber. The SWCNT incorporating into the P3HT-PEO fibers increased the conjugation length of the P3HT chains. Interaction between P3HT and CNT was confirmed by FTIR and Raman analysis. The charge transfer from P3HT to SWCNT was confirmed by Raman and photoluminescence analysis. At low SWCNT concentration into the P3HT-PEO fibers the conductivity was higher. A concentration of 0.4% SWCNT was determined as the most adequate to achieve a better dispersion of the SWCNT within the polymeric matrix P3HT-PEO. The P3HT-PEO-SWCNT fibers exhibited suitable properties to be applied in optoelectronic devices.

Acknowledgements The authors acknowledge to Dr. Judith C. Tanori Cordova for TEM analysis, Ing. Rogelio Morán Elvira for SEM Analysis, Dra. Mónica Acosta for Raman analysis and to CONACYT—México CB-2015/255512 and “FONDO SECTORIAL CONACYT-SENER-SUSTENTABILIDAD ENERGÉTICA” through the CEMIE-Sol/27 (Project No. 207450) for financial support.

Compliance with ethical standards

Conflict of interest The authors declare that they have no conflict of interest.

References

- Kuila BK, Park K, Dai L (2010) Soluble P3HT-grafted carbon nanotubes: synthesis and photovoltaic application. *Macromolecules* 43:6699–6705. <https://doi.org/10.1021/ma100917p>
- Bounioux C, Itzhak R, Avrahami R, Zussman E, Frey J, Katz EA, Yerushalmi-Rozen R (2011) Electrospun fibers of functional nanocomposites composed of single-walled carbon nanotubes, fullerene derivatives, and poly(3-hexylthiophene). *J Polym Sci Part B Polym Phys* 49:1263–1268. <https://doi.org/10.1002/polb.22281>
- Cai X, Zhu P, Lu X, Liu Y, Lei T (2017) Electrospinning of very long and highly aligned fibers. *J Mater Sci* 52:14004–14010. <https://doi.org/10.1007/s10853-017-1529-0>
- Katta P, Alessandro M, Ramsier RD, Chase GG (2004) Continuous electrospinning of aligned polymer nanofibers onto a wire drum collector. *Nano Lett* 4:2215–2218. <https://doi.org/10.1021/nl0486158>
- Lei T, Xu Z, Cai X, Xu L, Sun D (2018) New insight into gap electrospinning: toward meter-long aligned nanofibers. *Langmuir* 34:13788–13793. <https://doi.org/10.1021/acs.langmuir.8b03114>
- Kakade MV, Givens S, Gardner K, Lee KH, Chase DB, Rabolt JF (2007) Electric field induced orientation of polymer chains in macroscopically aligned electrospun polymer nanofibers. *J Am Chem Soc* 129(10):2777–2782. <https://doi.org/10.1021/acs.langmuir.8b03114>
- Bounioux C, Katz EA, Yerushalmi-Rozen R (2012) Conjugated polymers-carbon nanotubes-based functional materials for organic photovoltaics: a critical review. *Polym Adv Technol* 23(8):1129–1140. <https://doi.org/10.1002/pat.3054>
- Bounioux C, Díaz-Chao P, Campoy-Quiles M, Martín-González MS, Goni AR, Yerushalmi-Rozen R, Müller C (2013) Thermoelectric composites of poly(3-hexylthiophene) and

- carbon nanotubes with a large power factor. *Energy Environ Sci* 6(3):918–925. <https://doi.org/10.1039/c2ee23406h>
9. Hou H, Ge JJ, Zeng J, Li Q, Reneker DH, Greiner A, Cheng SZ (2005) Electrospun polyacrylonitrile nanofibers containing a high concentration of well-aligned multiwall carbon nanotubes. *Chem Mater* 17(5):967–973. <https://doi.org/10.1021/cm0484955>
 10. Abraham J, Sharika T, George SC, Thomas S (2017) Rheological percolation in thermoplastic polymer nanocomposites. *Rheol Open Access* 1:1–15
 11. Ponnamma D, Sadasivuni KK, Grohens Y, Guo Q, Thomas S (2014) Carbon nanotube based elastomer composites—an approach towards multifunctional materials. *J Mater Chem C* 2(40):8446–8485. <https://doi.org/10.1039/c4tc01037j>
 12. Akhina H, Gopinathan Nair MR, Kalarikkal N, Pramoda KP, Hui Ru T, Kailas L, Thomas S (2018) Plasticized PVC graphene nanocomposites: morphology, mechanical, and dynamic mechanical properties. *Polym Eng Sci* 58(S1):E104–E113. <https://doi.org/10.1002/pen.24711>
 13. Dror Y, Salalha W, Khalfin RL, Cohen Y, Yarín AL, Zussman E (2003) Carbon nanotubes embedded in oriented polymer nanofibers by electrospinning. *Langmuir* 19(17):7012–7020. <https://doi.org/10.1021/la034234i>
 14. Salalha W, Dror Y, Khalfin RL, Cohen Y, Yarín AL, Zussman E (2004) Single-walled carbon nanotubes embedded in oriented polymeric nanofibers by electrospinning. *Langmuir* 20(22):9852–9855. <https://doi.org/10.1021/la048536b>
 15. Ren S, Bernardi M, Lunt RR, Bulovic V, Grossman JC, Gradecak S (2011) Toward efficient carbon nanotube/P3HT solar cells: active layer morphology, electrical, and optical properties. *Nano Lett* 11(12):5316–5321. <https://doi.org/10.1021/nl202796u>
 16. Bar-Hen A, Bounioux C, Yerushalmi-Rozen R, Solveyra EG, Szeleifer I (2015) The role of steric interactions in dispersion of carbon nanotubes by poly (3-alkyl thiophenes) in organic solvents. *J Colloid Interf Sci* 452:62–68. <https://doi.org/10.1016/j.jcis.2015.04.038>
 17. Hernández-Martínez D, Martínez-Alonso C, Castillo-Ortega MM, Arenas-Arocena MC, Nicho ME (2015) Preparation and characterization of electrospun fibers containing poly (3-hexylthiophene) and poly (3-hexylthiophene)/CdS. *Synth Met* 209:496–501. <https://doi.org/10.1016/j.synthmet.2015.09.001>
 18. Samanta SK, Fritsch M, Scherf U, Gomulya W, Bisri SZ, Loi MA (2014) Conjugated polymer-assisted dispersion of single-wall carbon nanotubes: the power of polymer wrapping. *Acc Chem Res* 47(8):2446–2456. <https://doi.org/10.1021/ar500141j>
 19. Francis E, Ko HU, Kim JW, Kim HC, Kalarikkal N, Varughese K et al (2018) High-k dielectric percolative nanocomposites based on multiwalled carbon nanotubes and polyvinyl chloride. *J Mater Chem C* 6(30):8152–8159. <https://doi.org/10.1039/c8tc02528b>
 20. McCullough RD, Lowe RD, Jayaraman M, Anderson DL (1993) Design, synthesis, and control of conducting polymer architectures: structurally homogeneous poly (3-alkylthiophenes). *J Organ Chem* 58(4):904–912. <https://doi.org/10.1021/jo0056a024>
 21. Saini V, Li Z, Bourdo S, Dervishi E, Xu Y, Ma X et al (2009) Electrical, optical, and morphological properties of P3HT–MWNT nanocomposites prepared by in situ polymerization. *J Phys Chem C* 113(19):8023–8029. <https://doi.org/10.1021/jp809479a>
 22. Arici E, Karazhanov S (2016) Carbon nanotubes for organic/inorganic hybrid solar cells. *Mater Sci Semicond Process* 41:137–149. <https://doi.org/10.1016/j.mssp.2015.07.086>
 23. Alvarado-Tenorio G, Cortina-Marrero HJ, Nicho ME, Aguilar PM, Hu H (2016) Improvement of photovoltaic performance of inverted hybrid solar cells by adding single-wall carbon nanotubes in poly (3-hexylthiophene). *Mater Sci Semicond Process* 56:37–42. <https://doi.org/10.1016/j.mssp.2016.07.018>
 24. Li J, Aoki K (1998) Electrochemical gelation of poly (3-hexylthiophene) film. *J Electroanal Chem* 453(1–2):107–112. [https://doi.org/10.1016/S0022-0728\(98\)00238-1](https://doi.org/10.1016/S0022-0728(98)00238-1)
 25. Singh RK, Kumar J, Singh R, Kant R, Chand S, Kumar V (2007) Micromorphology, photophysical and electrical properties of pristine and ferric chloride doped poly (3-hexylthiophene) films. *Mater Chem Phys* 104(2–3):390–396. <https://doi.org/10.1016/j.matchemphys.2007.01.024>
 26. Hotta S, Rughooputh SDDV, Heeger AJ, Wudl F (1987) Spectroscopic studies of soluble poly (3-alkylthiophenes). *Macromolecules* 20(1):212–215. <https://doi.org/10.1021/ma00167a038>
 27. Su YL, Wang J, Liu HZ (2002) Melt, hydration, and micellization of the PEO–PPO–PEO block copolymer studied by FTIR spectroscopy. *J Colloid Interface Sci* 251(2):417–423. <https://doi.org/10.1006/jcis.2002.8435>
 28. López-Mata C, Nicho ME, Altuzar-Coello P, del Angel-Meraz E, García-Escobar CH, Cadenas-Pliego G (2015) Synthesis and characterization of SWNTs/P3OT composites via in situ microwave-assisted polymerization. *J Mater Sci Mater Electron* 26:7341–7350. <https://doi.org/10.1007/s10854-015-3363-y>
 29. Musumeci AW, Silva GG, Liu JW, Martens WN, Waclawik ER (2007) Structure and conductivity of multi-walled carbon nanotube/poly (3-hexylthiophene) composite films. *Polymer* 48(6):1667–1678. <https://doi.org/10.1016/j.polymer.2007.01.027>
 30. Chen TA, Wu X, Rieke RD (1995) Regiocontrolled synthesis of poly(3-alkylthiophenes) mediated by Rieke Zinc: their characterization and solid-state properties. *J Am Chem Soc* 117:233–244. <https://doi.org/10.1021/ja00106a027>
 31. Karim MR (2012) Synthesis and characterizations of poly (3-hexylthiophene) and modified carbon nanotube composites. *J Nanomater*. <https://doi.org/10.1155/2012/174353>
 32. Eklund PC, Holden JM, Jishi RA (1996) Vibrational modes of carbon nanotubes; spectroscopy and theory. In: Endo M, Iijima S, Dresselhaus MS (eds) *Carbon nanotubes*. Pergamon, Oxford, pp 129–142. <https://doi.org/10.1016/B978-0-08-042682-2.50020-5>
 33. Meng D, Sun J, Jiang S, Zeng Y, Li Y, Yan S et al (2012) Grafting P3HT brushes on GO sheets: distinctive properties of the GO/P3HT composites due to different grafting approaches. *J Mater Chem* 22(40):21583–21591. <https://doi.org/10.1039/c2jm35317b>
 34. Patel RJ, Tighe TB, Ivanov IN, Hickner MA (2011) Electro-optical properties of electropolymerized poly (3-hexylthiophene)/carbon nanotube composite thin films. *J Polym Sci Part B Polym Phys* 49:1269–1275. <https://doi.org/10.1002/polb.22307>
 35. Goutam PJ, Singh DK, Iyer PK (2012) Photoluminescence quenching of poly (3-hexylthiophene) by carbon nanotubes. *J Phys Chem C* 116(14):8196–8201. <https://doi.org/10.1021/jp300115q>

Publisher's Note Springer Nature remains neutral with regard to jurisdictional claims in published maps and institutional affiliations.